

Canonical and Microcanonical Calculations for Fermi Systems

Scott Pratt

*Department of Physics and Astronomy and
National Superconducting Cyclotron Laboratory,
Michigan State University, East Lansing, MI 48824 USA*

(May 11, 2018)

Abstract

Recursion relations are presented that allow exact calculation of canonical and microcanonical partition functions of degenerate Fermi systems, assuming no explicit two-body interactions. Calculations of the level density, sorted by angular momentum, are presented for ^{56}Ni . The issue of treating unbound states is also addressed.

Statistical models have played a central role in the study of the nucleus since Bohr's model of the compound nucleus in 1936 [1,2]. Level densities and occupation probabilities are important in determining reaction rates at finite temperature in astrophysical studies [3] and heavy-ion reactions [4]. Level densities also dominate the behavior of low-energy neutron scattering [5]. A nearly identical set of problems appears in atomic physics when modeling highly excited electronic configurations in heavier atoms. There, level densities and occupation probabilities play a pivotal role in understanding the opacity of interstellar dust which affects the interpretation of a variety of astrophysical measurements [6,7]. Mesoscopic systems are also beginning to play an increasingly important role in other fields, such as the study of quantum dots or atomic clusters. In this letter, we present methods to perform exact calculations of both canonical and microcanonical quantities. These methods involve the counting of all possible arrangements of fermions amongst independent single-particle levels. We apply these methods to the example of counting levels in ^{56}Ni . Even though explicit residual interactions are ignored, the methods allow insight into a variety of problems involving finite Fermi systems. We also discuss possible extensions of these pictures that would treat residual interactions.

The calculations presented here are based on recursive algorithms. The algorithms can be considered as extensions to techniques used for multi-particle symmetrization which has been applied in the context of heavy ion collisions for both Bose and Fermi systems [8,9] and extended to weakly interacting Bose gases [10]. The simplest application considers the canonical partition function, Z_A , for a system of A identical fermions populating a finite set of energy levels, ϵ_i , at an inverse temperature β .

$$Z_A(\beta) = \frac{1}{A!} \sum_{j_1 \cdots j_A, \mathcal{P}(j)} \langle j_1 \cdots j_A | e^{-\beta H} | \mathcal{P}(j_1 \cdots j_A) \rangle. \quad (1)$$

Here, the A particles are treated as distinguishable. They occupy the states, j_1, \dots, j_A which are eigenstates of H , and $\mathcal{P}(j)$ refers to the $A!$ permutations of $j_1 \cdots j_A$.

The permutations may be categorized diagrammatically. As an example, a 9-particle permutation is illustrated in Fig. 1, where the n^{th} position in the permutation is found by

following the segment of the loop that leaves from the n^{th} site on the diagram. The sum over diagrams represents the sum over permutations, and a given closed loop represents a permutation cycle.

$$C_n = \sum_i e^{-n\beta\epsilon_i} (-1)^{n-1}. \quad (2)$$

All diagrams can be expressed as a product of cycles. The diagram written in Fig. 1 may be expressed as the product, $C_1 C_2^2 C_4$. The sign $(-1)^{n-1}$ arises from the number of pairwise permutations required to create the loop, and is ignored in the case of Bosons.

One may now derive the recursion relation for the partition function by considering summing over diagrams according to the cycle of the loop connecting the upper left point.

$$\begin{aligned} Z_A(\beta) &= \frac{1}{A!} \left(\sum \text{ all diagrams of order } A \right) \\ &= \frac{1}{A!} \sum_n \frac{(A-1)!}{(A-n)!} C_n \left(\sum \text{ all diagrams of order } A-n \right) \\ &= \frac{1}{A} \sum_n C_n Z_{A-n}(\beta) \end{aligned} \quad (3)$$

The factor $(A-1) \cdots (A-n+1)$ in the second line of Eq. (3) may be understood by counting the number of ways in which a loop of size n may be connected to one point.

Eq. (3) allows practically instantaneous calculation of the partition function given the single-particle energy levels ϵ_i . This approach also leads to a simple expression for two-point functions,

$$\langle a_i^\dagger a_j \rangle = \delta_{ij} \frac{1}{Z_A(\beta)} \sum_n e^{-n\beta\epsilon_i} (-1)^{n-1} Z_{A-n}(\beta). \quad (4)$$

The four-point function might also be of interest in calculations of residual interactions.

$$\langle a_i^\dagger a_j^\dagger a_k a_l \rangle = \frac{1}{Z_A(\beta)} (\delta_{il} \delta_{jk} - \delta_{ik} \delta_{jl}) \sum_{n_i, n_j} e^{-n_i \beta \epsilon_i - n_j \beta \epsilon_j} (-1)^{n_i + n_j} Z_{A-n_i-n_j}(\beta) \quad (5)$$

It is straight-forward to extend these calculations to arbitrary n -point functions.

The method is easily extended to include conserved quantities. For instance, conservation of the z -component of angular momentum J_z can be accommodated by summing over only those diagrams which yield a fixed sum, $M = \sum_i n_i m_i$.

$$Z_{A,M}(\beta) = \frac{1}{A} \sum_{n,i} e^{-n\beta\epsilon_i} (-1)^{n-1} Z_{A-n,M-nm_i}(\beta) \quad (6)$$

In a similar fashion one may incorporate any other conservation laws, such as parity, by adding an additional subscript to Z .

By setting β to zero, one may associate Z with a counting of all states regardless of energy. By setting $\beta = 0$, and assigning a discretized energy to each state, one may count the net number of states with total energy E .

$$N_{A,E,M} = \frac{1}{A} \sum_{n,i} (-1)^{n-1} N_{A-n,E-n\epsilon_i,M-nm_i}. \quad (7)$$

The above relation requires that energy be measured in discrete units. These units can be arbitrarily small to make the calculation approach the continuum limit. The quantity N represents the microcanonical partition function, and when divided by the energy bin size, yields the density of states.

One may also calculate the microcanonical equivalent of the two and four-point functions.

$$\langle a_i^\dagger a_j \rangle = \delta_{ij} \frac{\sum_n (-1)^{n-1} N_{A-n,E^*-n\epsilon_i,M-nm_i}}{N_{A,E^*,M}} \quad (8)$$

$$\langle a_i^\dagger a_j^\dagger a_k a_l \rangle = (\delta_{il} \delta_{jk} - \delta_{ik} \delta_{jl}) \frac{\sum_{n_i n_j} (-1)^{n_i+n_j} N_{A-n_i-n_j,E^*-n_i\epsilon_i-n_j\epsilon_j,M-n_i m_i-n_j m_j}}{N_{A,E^*,M}} \quad (9)$$

Calculations proceed more quickly when particles and holes are considered independently, then convoluted to find the number of states at a fixed E^* and M . Considering only states with energies above the Fermi level, one first finds $N_{a,E^*,M}^p$, the number of ways to arrange a particles above the Fermi surface such that they sum to energy E^* and angular momentum projection M . Then, considering only states below the Fermi surface, one performs the analogous calculation for a holes, $N_{a,E^*,M}^h$. The number of ways to arrange particles and holes subject to conservation of particle number, energy and angular momentum is

$$N_{E^*,M} = \sum_{a,E',M'} N_{a,E'-E_f,M-M'}^p N_{a,E^*-(E'-E_f),M'}^h. \quad (10)$$

Instead of counting states with a specific projection $M = \langle J_z \rangle$, one may count \tilde{N}_J , the number of multiplets of a given J , by converting the recursion relations for N_M into a relation for \tilde{N}_J .

$$\tilde{N}_J = N_J - N_{J+1} \quad (11)$$

$$N_M = \sum_{J \geq |M|} \tilde{N}_J$$

By manipulating Eq. (7) and Eq.s (11), one may derive a recursion relation for \tilde{N}_J .

$$\tilde{N}_{A,J,E} = \sum_{n,i} (-1)^{n-1} \sum_{-j_i \leq m_i \leq j_i} \left(\tilde{N}_{A-n,J-nm_i,E-n\epsilon_i} \Theta(J - nm_i) - \tilde{N}_{A-n,nm_i-J-1,E-n\epsilon_i} \Theta(nm_i - J - 1) \right), \quad (12)$$

where the sum over i represents a sum over multiplets of a given j rather than a sum over individual states.

The simplest example to consider is that of equally-spaced non-degenerate levels which was addressed by Ericson [11]. This example can be related to the problem of finding the number of ways an integer can be written as a sum of smaller integers without using the same integer twice. The resulting density of states which is displayed in Fig. (4) is well matched by the Bethe formula [12,13],

$$\rho(E) \approx \frac{\exp\left(2\pi\sqrt{gE^*/6}\right)}{\sqrt{48E^*}}, \quad (13)$$

where g is the single-particle level density and E^* is the excitation energy above the ground state. Fig. 3 displays the two-point function, $f_i = \langle a_i^\dagger a_i \rangle$ at a fixed excitation energy of $20 g^{-1}$. The resulting phase space filling factor is fairly well described by a Fermi function, represented by a solid line in Fig. 3, with the temperature set at $T = \sqrt{\frac{6E^*}{\pi^2 g}}$.

We now consider a more realistic example where single-particle levels for ^{56}Ni were generated from a Hartree-Fock calculation [14]. An infinite external potential was added to confine the particles to within a 10 fm sphere, transforming the continuum into a set of densely packed discrete states. All levels within 50 MeV of the Fermi surface were included. The lowest 20 single-particle energy levels are listed in Table I.

TABLES

TABLE I. Single-particle energy levels of ^{56}Ni from Hartree-Fock calculations in MeV.

level	Proton	Neutron	level	Proton	Neutron
$s_{1/2}$	-32.59	-42.61	$g_{9/2}$	3.93	-5.33
$p_{3/2}$	-24.23	-34.10	$d_{5/2}$	8.17	-0.53
$p_{1/2}$	-22.56	-32.48	$d_{3/2}$	9.36	0.94
$d_{5/2}$	-15.33	-25.04	$s_{1/2}$	9.41	1.32
$s_{1/2}$	-11.46	-21.28	$g_{7/2}$	12.11	3.30
$d_{3/2}$	-11.10	-20.87	$h_{11/2}$	14.37	5.52
$f_{7/2}$	-6.01	-15.53	$p_{3/2}$	21.42	7.68
$p_{3/2}$	-1.90	-11.41	$p_{1/2}$	14.53	8.16
$p_{1/2}$	-0.52	-9.92	$f_{7/2}$	14.95	8.66
$f_{5/2}$	0.80	-8.67	$f_{5/2}$	15.92	10.00

The Fermi energy was set at -15.5 MeV for neutrons and -6.0 MeV for protons. The energy was discretized in units of 0.25 MeV. One may then couple the resulting level density for neutrons with the proton level density to obtain the level density of the composite system.

Figure 4 displays the resulting density of states for three cases. First, the density of states is displayed for the case where all single-particle levels are included, even those that are unbound. Secondly, results are shown for a calculation where only the fp and $g_{9/2}$ shells are considered, as was implemented in a Monte Carlo shell-model calculation of Nakada and Alhassid [15]. Ormand [16], Langanke [17] and Dean [18] have performed similar studies.

Continuum levels should not be included in the treatment [19]. Therefore, the recursive sums were modified to subtract the contribution from the continuum in the following manner,

$$N_{A,E} = \frac{1}{A} \sum_n (-1)^{n-1} \left(\sum_i N_{A-n,E-\epsilon_i} - \sum_{i'} N_{A-n,E-\epsilon_{i'}} \right), \quad (14)$$

where the primed sums are over eigenstates of the infinite confining spherical well without interactions. In the limit that the radius of the confining well approaches infinity, the correction should be exact. Figure 4 displays the corrected level density for the ^{56}Ni example. The correction only becomes substantial above excitations of 25 MeV. At lower energies the aforementioned subset of levels seems sufficient to reproduce the density of states.

Figure 5 displays the number of multiplets within specified energy windows for ^{56}Ni as a function of J . Describing the coupling of angular momentum as a diffusive random walk [11], one expects the J dependence to behave as

$$N_{E,J} \propto (J + \frac{1}{2}) \exp -\beta J(J + 1), \quad (15)$$

where β is related to the number of particles and the average j of the single-particle levels used to form the angular momentum [11]. As seen in Fig. 5 where β was chosen to best fit the results, the functional form is accurate except at high J .

The recursion relations presented here appear quite powerful in calculating statistical quantities of excited nuclei with minimal calculational time. The method may easily accommodate an arbitrarily large number of single-particle levels. The ^{56}Ni calculations required

approximately 5 minutes of CPU time on a low-end workstation, and most of that time was spent performing the coupling of particles to holes described in Eq. (10). Enumeration of states and their angular momentum is required for nuclear shell-model calculations. In current shell-model codes, this is accomplished by combinatorially considering all ways in which n particles can be placed into m states. These methods are sufficient as long as a small number of single-particle levels are involved. For large nuclei or as one enters or approaches the continuum, the number of single-particle levels becomes large and the benefits of the recursive method are more apparent. Since the recursive method yields partition functions, it is straight-forward to extend it to the calculation of any statistical quantity.

Although the relations are flexible in handling any model given the single-particle levels, two-body (residual) interactions are explicitly ignored. However, they can be included perturbatively. For example, four-point terms can be calculated using Eq.s (5) and (9). The four-point terms can then be used to calculate the contribution of the residual interaction in lowest order. It is our hope that the recursive techniques presented here might be expanded to include a framework for calculating successively higher order perturbations.

ACKNOWLEDGMENTS

The author wishes to thank Vladimir Zelevinsky, Alex Brown and Declan Mulhall for sharing their expertise. This work was support by the National Science Foundation, PHY-96-05207.

REFERENCES

- [1] N. Bohr, *Nature* **137**, 344 (1936).
- [2] V.F. Weisskopf, *Phys. Rev.* **52**, 295 (1937).
- [3] T. Rauscher, F.-K. Thielemann and K.-L. Kratz, *Phys. Rev. C* **56**, 1613 (1997).
- [4] W.A. Friedman, *Phys. Rev. C* **42**, 667 (1990).
- [5] C.M. Frankle, E.I. Sharapov, Yu.P. Popov, J.A. Harvey, N.W. Hill and L.W. Weston, *Phys. Rev. C* **50**, 2774 (1994).
- [6] Opacity Project Team, *The Opacity Project*, Vol. 1, Inst. of Phys. Publishing, Bristol, ISBN 0-7503-0288-7 (1995).
- [7] M.J. Seaton, Y. Yan, D. Mihalas, A.K. Pradhan, *NNRAS* **266**, 805 (1994).
- [8] S. Pratt, *Phys. Lett. B* **301**, 159 (1993).
- [9] S. Pratt and W. Bauer, *Phys. Lett. B* **329**, 413 (1994).
- [10] K.C. Chase, A.Z. Mekjian and L. Zamick, *Eur. Phys. J. B* **8**, 281 (1998).
- [11] T. Ericson, *T. Adv. in Physics* **9**, 425 (1960).
- [12] H. Bethe, *Phys. Rev.* **50**, 332 (1936); *Phys. Rev.* **53**, 675 (1938).
- [13] A. Bohr and B.R. Mottleson, Nuclear Structure, Vol. 1, World Scientific (1998).
- [14] B.A. Brown, *Phys. Rev. C* **58**, 220 (1998).
- [15] N. Nakada and Y. Alhassid, *Phys. Rev. Lett.* **79**, 2939 (1997); *Phys. Lett. B* **436**, 3468 (1998).
- [16] W.E. Ormand, *Phys. Rev. C* **56**, R1678 (1997).
- [17] K. Langanke, *Phys. Lett. B* **438**, 235 (1998).
- [18] D. Dean and S.E. Koonin, LANL report, nucl-th/9902067 (1999).

[19] S. Shlomo, V.M. Kolomietz and H. Dejbakhsh, Phys. Rev. C**55**, 1972 (1997).

FIGURES

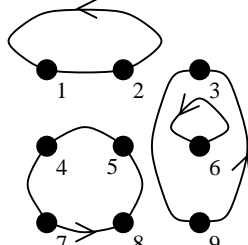


FIG. 1. A sample permutation is represented by the diagram above. The permutation of $j_1 \dots j_9$ in this case is $j_2, j_1, j_9, j_7, j_4, j_6, j_8, j_5, j_3$ as the segment leaving the dot labeled n , is connected to j'_n in the permutation. This diagram can be expressed in terms of cycles by $C_1 C_2^2 C_4$.

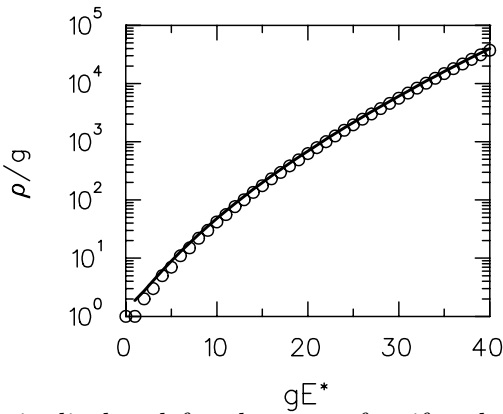


FIG. 2. The level density is displayed for the case of uniformly spaced levels. It is well approximated by the Bethe formula when the excitation energy is much greater than the inverse single-particle level spacing, g^{-1} .

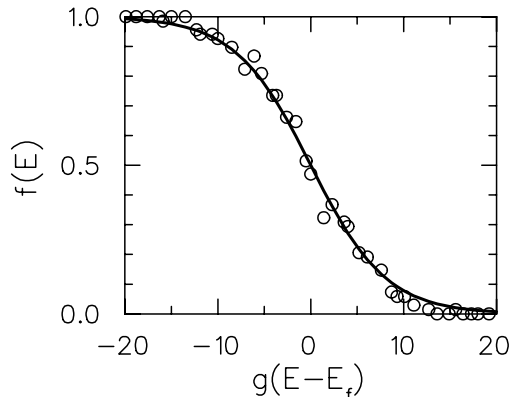


FIG. 3. The occupation probability is shown for the case of uniformly-spaced levels where the energy is fixed at 10 times the single-particle level spacing.

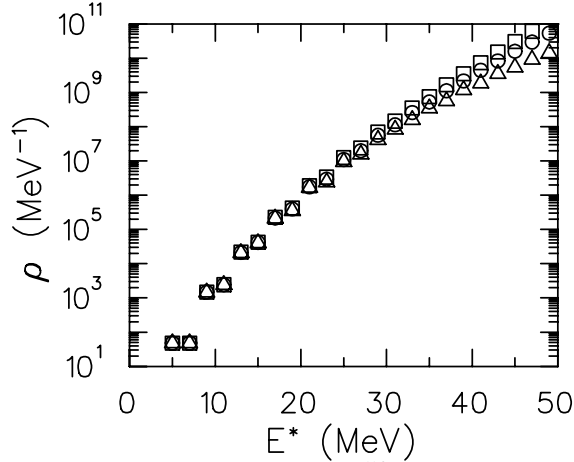


FIG. 4. Calculations for the density of states for ^{56}Ni are displayed for three sets of states.

Results which consider only fp and the $g_{9/2}$ shell are represented by triangles, including all states is represented by squares, while subtracting continuum corrections yields the results represented by circles.

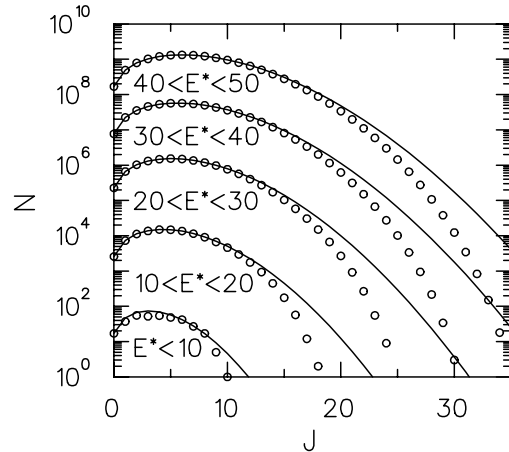


FIG. 5. The number of multiplets of a given J for ^{56}Ni are shown for the energy windows labeled above. The fits to the form shown in Eq. (15) are shown with lines. The form well describes the result, except for high J .